Black Sea Journal of Engineering and Science
doi: 10.34248/bsengineering.1695365

Open Access Journal
e-ISSN: 2619 – 8991

Research Article
Volume 8 - Issue 4: 1195-1203 / July 2025

MICROSTRUCTURAL EVOLUTION AND RADON EMISSION DYNAMICS IN CLASS F FLY ASH-BLENDED CEMENT PASTES

Ahmad HOSSEINPOUR SHEIKHRAJAB[1*], Ahmet ERDAL OSMANLIOĞLU[1]

[1]Istanbul University-Cerrahpaşa, Faculty of Engineering, Department of Mining Engineering, 34500, Istanbul, Türkiye

Abstract: Radon release from cementitious building materials is a major indoor air quality concern due to the presence of naturally occurring radionuclides in raw materials. This study investigates the influence of partially replacing Portland cement with Class F coal fly ash (0–50% by weight) on the pore structure and radon emission of hardened cement pastes. Cement paste specimens with varying fly ash content were analyzed using mercury intrusion porosimetry (MIP) to quantify porosity and pore size distribution, and an open-loop radon concentration setup (using a DURRIDGE RAD7 detector) to measure radon exhalation. The results reveal that increasing fly ash content leads to a pronounced increase in total porosity (from 14.23% at 0% fly ash to 20.22% at 50% replacement) and a corresponding rise in radon concentration (steady-state radon concentrations increasing from 20.8 Bq/m^3 to 32.1 Bq/m^3 for the same range). Microstructural analysis indicates that high fly ash substitution coarsens the pore network – the volume-based median pore diameter expanded from ~102 nm to ~381 nm – while also nearly doubling the internal surface area, reflecting the development of both larger capillary voids and fine pores. These changes suggest enhanced radon transport pathways at higher fly ash levels. The findings underscore a mechanistic link between fly ash-induced pore structure modifications and radon diffusion behavior. High-volume fly ash use, while beneficial for sustainability and reduced clinker usage, can thus inadvertently increase radon release. Therefore, optimizing the replacement ratio is essential to balance sustainability goals with indoor air quality considerations and to minimize potential health risks associated with indoor radon exposure.

Keywords: Radon emission, Fly ash, Cement paste, Microstructure, Porosity, Sustainability

***Corresponding author:** Istanbul University-Cerrahpaşa, Faculty of Engineering, Department of Mining Engineering, 34500, Istanbul, Türkiye
E mail: ahmad.hosseinpour50@gmail.com (A. HOSSEINPOUR SHEIKHRAJAB)
Ahmad HOSSEINPOUR SHEIKHRAJAB https://orcid.org/0009-0001-0132-3026
Ahmet ERDAL OSMANLIOĞLU https://orcid.org/0000-0001-5547-7525

Received: May 08, 2025
Accepted: July 01, 2025
Published: July 15, 2025

Cite as: Hosseinpour Sheikhrajab A, Osmanlıoğlu AE. 2025. microstructural evolution and radon emission dynamics in class F fly ash-blended cement pastes. BSJ Eng Sci, 8(4): 1195-1203.

1. Introduction

Radon is a radioactive noble gas that arises naturally from the decay of uranium and thorium found in the earth's crust, including soils, rocks, and some construction materials. Among its isotopes, Radon-222 (Rn-222) is of particular concern in indoor settings due to its relatively long half-life of 3.8 days and its origin from the decay of radium-226 (Ra-226), which is commonly present in natural materials like fly ash. Being colorless, odorless, and chemically inert, radon can migrate through soil and porous building materials, accumulating in enclosed environments such as basements and poorly ventilated rooms. As a Group 1 carcinogen, radon is the second leading cause of lung cancer after tobacco use, primarily due to its alpha-emitting decay products, such as polonium-218 and lead-214, which can damage lung tissue upon inhalation (EPA, 2023; Field et al., 2007; World Health Organization, 2010). To mitigate associated health risks, international organizations have proposed exposure limits. The World Health Organization (WHO) recommends a reference level of 100 Bq/m^3 for indoor radon, while the U.S. Environmental Protection Agency (EPA) has set an action level of 148 Bq/m^3. These thresholds are critical for assessing indoor air quality and guiding ventilation and material selection practices in buildings. Buildings can become entry points for radon through structural pathways like cracks in foundations, but building materials themselves may also release radon, especially if they contain trace amounts of naturally occurring radioactive materials (NORM)(Righi and Bruzzi, 2006). Portland cement is one such material, and when it is partially replaced with industrial by-products like fly ash—a residue generated from coal-fired power plants—its radiological and structural characteristics can change. Although fly ash is valued for its economic and environmental benefits (Yüksel and Göncüoğlu, 2011), it often contains elevated concentrations of uranium and thorium, leading to concerns about its potential to increase radon concentrations in indoor environments (Blissett, 2012; Mehta and Monteiro, 2014; Osmanlıoğlu, 2019).

Some studies associate the use of fly ash with increased radon release due to its higher radionuclide content. Others highlight a decrease in radon emissions, attributing the reduction to the microstructural changes that fly ash introduces—particularly in pore structure and radon transport behavior (Kumar, Chauhan, and

This work is licensed (CC BY-NC 4.0) under Creative Commons Attribution 4.0 International License

Dahiya, 2010; Osmanlıoğlu, 2021; Zhang and Malhotra, 1996). Given that factors like pore size, porosity, and interconnectivity play a major role in controlling gas transport and retention, the relationship between fly ash content and radon behavior is influenced both by the intrinsic radioactivity of the material and by the microstructural changes it induces.

This research aims to investigate how the partial substitution of Portland cement with fly ash impacts both the porosity and radon emission characteristics of hardened cement pastes. The fly ash used in this study, sourced from the Tunçbilek Thermal Power Plant in Turkey, represents a typical example of lignite-based ash with naturally elevated radioactivity (Hosseinpour, 2025). By preparing cement pastes with six fly ash substitution levels (0%, 5%, 10%, 15%, 30%, and 50%) and analyzing them through mercury intrusion porosimetry and open-loop radon measurements using the DURRIDGE RAD7 system, the study aims to clarify the relationship between pore structure development and radon release.

Ultimately, this study contributes to a better understanding of how fly ash can be strategically utilized in cementitious systems to enhance sustainability while identifying its potential radiological implications. Since fly ash modifies both the radionuclide content and the pore structure of hardened pastes, the level of substitution must be carefully optimized. Higher replacement ratios may increase radon emission due to both enhanced radium content and greater pore connectivity, potentially raising indoor exposure risks. These findings underscore the need to balance environmental benefits with public health considerations in sustainable construction.

2. Materials and Methods

2.1. Study Objective and Experimental Scope

This research focuses on assessing the influence of replacing Portland cement with fly ash on the porosity, pore structure, and radon emission characteristics of cement pastes. To this end, a detailed experimental procedure was followed, encompassing raw material analysis, preparation of samples with varying levels of fly ash, porosity characterization using mercury intrusion porosimetry, and radon concentration testing through an open-loop setup utilizing a RAD7 radon detector.

2.2. Materials Used

2.2.1. Portland cement

The cement employed in this study was Portland cement (CEM I 42.5 R), supplied by Akçansa Cement Factory. Essential physicochemical properties such as specific gravity, Blaine fineness, and radionuclide content (including uranium and thorium concentrations) were determined and presented in Table 1.

2.2.2. Reference sand

The fine aggregate used was CEN standard reference sand, obtained from Limak Trakya Cement Factory. It is composed of high-purity, rounded silica particles. The aggregate's physical characteristics and radiological content are summarized in Table 2.

2.2.3. Fly ash

Class F fly ash, in compliance with ASTM C618, was sourced from the Tunçbilek Thermal Power Plant (Hosseinpour and Osmanlıoğlu, 2024). This byproduct of coal combustion was analyzed for fineness, oxide composition, and radioactive element concentration. The corresponding results are provided in Table 3.

Table 1. Cement properties

Parameter	Value	Unit	Test Method	Standard Reference
Uranium (U) Concentration	3	ppm	IHM (in-house method)	N/A (lab internal method)
Thorium (Th) Concentration	1.79	ppm	In-house (IHM) procedure for Th content	N/A (lab internal method)
Specific Gravity	2.69	–	Displacement (Le Chatelier flask method)	TS EN 196-6:2020
Grain Density	3.10	g/cm^3	Gas pycnometry	ASTM C604 (Helium pycnometer)
Fineness (90 µm sieve residue)	20	%	Dry sieving (90µm mesh)	TS EN 196-6:2020

Table 2. Sand properties

Parameter	Value	Unit	Test Method	Standard Reference
Uranium (U)	0.53	ppm	IHM (in-house method)	N/A* (lab internal method)
Thorium (Th)	2.40	ppm	IHM (in-house method)	N/A (lab internal method)
Specific Gravity	2.29	g/cm^3	Pycnometric Density (Pulp)	N/A (lab internal method)

*N/A= Not applicable.

Table 3. Fly ash properties

Parameter	Value	Unit	Test Method	Standard Reference
Uranium (U)	8.37	ppm	IHM (in-house method)	N/A (lab internal method)
Thorium (Th)	29.06	ppm	IHM (in-house method)	N/A (lab internal method)
Specific Gravity	2.20	g/cm^3	Pycnometric Density (Pulp)	N/A (lab internal method)
Fineness (45 µm residue)	19	%	Wet sieving	EN 450-1
Silicon Dioxide (SiO_2)	54.79	% (w/w)	TS EN 15309:2007	EN 15309
Aluminum Oxide (Al_2O_3)	18.58	% (w/w)	TS EN 15309:2007	EN 15309
Iron Oxide (Fe_2O_3)	8.90	% (w/w)	TS EN 15309:2007	EN 15309
Calcium Oxide (CaO)	2.81	% (w/w)	TS EN 15309:2007	EN 15309

2.3. Sample preparation and testing protocols

Cement paste specimens were prepared in line with TS EN 196-1 specifications. Different mix designs were developed by partially substituting Portland cement with fly ash at 0%, 5%, 10%, 15%, 30%, and 50% by mass. All mixes maintained a constant binder-to-sand ratio of 1:3 and a fixed water-to-binder (w/b) ratio (0.5) to ensure consistency in workability and hydration conditions.

For porosity measurements, six prismatic specimens measuring 160 × 40 × 40 mm were cast and cured for 28 days prior to testing. Additionally, six cylindrical specimens with dimensions of 48 mm in diameter and 51 mm in height were prepared for radon emission analysis. Three separate raw material samples were also fabricated to assess radon concentrations. The classification, mixture proportions, and dimensions of all specimens are summarized in Table 4, while their physical appearance is presented in Figure 1. In total, fifteen samples were tested, encompassing the control mix, fly ash-modified cement pastes, and individual raw material references.

Table 4. Nomenclature of produced samples, mixture ratios, and sizes

Sample Name	% Cement + %Fly ash (% by weight) (gr)	Sand (gr)	Water (gr)	Sample Size (mm)
FL0	% 100 Cement (150 gr) + % 0 Fly ash	450	75	40x40x160
FL5	% 95 Cement (142.5 gr) + % 5 Fly ash (7.5 gr)	450	75	40x40x160
FL10	% 90 Cement (140 gr) + % 10 Fly ash (10 gr)	450	75	40x40x160
FL15	% 85 Cement (127.5 gr) + % 15 Fly ash (22.5 gr)	450	75	40x40x160
FL30	% 70 Cement (105 gr) + % 30 Fly ash (45 gr)	450	75	40x40x160
FL50	% 50 Cement (75 gr) + % 50 Fly ash (75 gr)	450	75	40x40x160
CL0	% 100 Cement (44.5 gr) + % 0 Fly ash	133.3	22.22	*R=48mm H=51mm
CL5	% 95 Cement (42.28gr) + % 5 Fly ash (2.22 gr)	133.3	22.22	R=48mm H=51mm
CL10	% 90 Cement (40.5 gr) + % 10 Fly ash (4.45 gr)	133.3	22.22	R=48mm H=51mm
CL15	% 85 Cement (37.83 gr) + % 15 Fly ash (6.67 gr)	133.3	22.22	R=48mm H=51mm
CL30	% 70 Cement (31.15 gr) + % 30 Fly ash (13.35 gr)	133.3	22.22	R=48mm H=51mm
CL50	% 50 Cement (22.5 gr) + % 50 Fly ash (22.5 gr)	133.3	22.22	R=48mm H=51mm
P1	Cement (180 gr) + Fly ash (0 gr)	0	0	Powder
P2	Cement (0 gr) + Fly ash (180gr)	0	0	Powder
P3	Cement (0 gr) + Fly ash (0 gr)	133.33	0	Aggregate

*R= Cylinder diameter. H= Cylinder height.

Figure 1. Physical appearance of the control, fly ash-modified cement pastes, and raw material specimens.

Porosity characterization was carried out using a Micromeritics AutoPore IV mercury intrusion porosimeter. This method involves the application of pressurized mercury to quantify pore volume and distribution, following the Washburn equation and Laplace's law (Diamond, 2000). The device measured pore diameters ranging from approximately 3.6 nm to 1000 µm. Parameters obtained included total pore volume (mL/g), surface area (m^2/g), volume- and area-based median pore diameters, average pore diameter (4V/A), bulk density, skeletal density, and total porosity percentage.

Prior to analysis, cement paste specimens were oven-dried at 50 °C for 48 hours in order to preserve their pore structures. Once dried, the samples were crushed into fragments smaller than 4 mm, suitable for mercury intrusion porosimetry (MIP). The tests were performed using a penetrometer with a stem volume of 1.1310 mL and a total penetrometer volume of 6.6790 mL. Mercury intrusion was conducted within a pressure range from 0.52 psia (filling pressure) to 4.45 psia (maximum applied pressure), enabling the assessment of pore diameters ranging from approximately 100 µm down to 3 nm. The porosity test is shown in Figure 2.

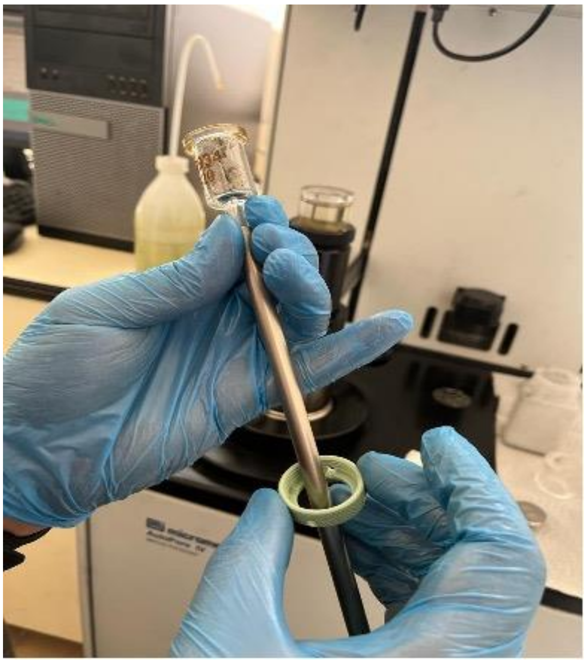

Figure 2. The porosity test.

Radon emission testing was conducted using a DURRIDGE RAD7 detector configured in an open-loop system. Each cylindrical hardened specimen was placed inside an airtight chamber equipped with two valves—one connected to the RAD7 inlet to draw air continuously and the other left open to allow ambient air to enter (Figure 3). Operating in Sniff Mode, the RAD7 —an active and continuous radon monitoring device—recorded radon levels at five-minute intervals over periods ranging from 1.7 to more than 3 days, producing between 500 and 999 data points per sample. This setup enabled consistent internal air circulation and facilitated accurate tracking of radon release over time. The continuous five-minute interval recordings allowed for the observation of temporal emission patterns, including the initial accumulation phase and the eventual stabilization behavior. The background radon concentration in the laboratory, measured at 19 Bq/m^3, was used as a reference for comparison. Each radon emission test was conducted in triplicate under identical environmental conditions. The mean values and corresponding standard deviations were calculated and presented in Table 6 to indicate measurement consistency and data reliability.

Figure 3. Open loop radon concentration test.

The same experimental setup was employed to assess radon emissions from individual raw materials—cement, fly ash, and aggregate. These were placed in identical sealed containers with dual valves, as depicted in Figure 1, and analyzed using the same open-loop protocol. Figure 3 displays open loop radon concentration test.

The time-based measurements showed that radon levels increased during the first hours and eventually stabilized, indicating that emission reaches a near-steady state under open-loop conditions. This behavior aligns with prior studies and supports the reliability of the measurement technique.

3. Results

3.1. Porosity and pore structure results

The mercury intrusion porosimetry (MIP) analyses showed a consistent increase in total porosity, pore volume, and internal surface area with higher levels of fly ash substitution in the cement pastes. According to the results (Table 5), porosity rose from 14.23% in the reference mix (0% fly ash) to 20.22% at the 50% substitution level. Similarly, the total pore volume increased from 0.0664 to 0.1005 mL/g. A notable rise in total pore surface area was also recorded, from 5.825 m^2/g to 10.481 m^2/g, nearly doubling across the substitution range.

Moreover, the distribution of pore sizes shifted significantly. The volume-based median pore diameter increased from 102.3 nm to 380.7 nm, indicating a growing fraction of larger capillary pores. In contrast, the area-based median pore diameter dropped from 14.7 nm to 5.4 nm.

Table 5. The mercury intrusion porosimetry (MIP) analyses results

Sample Name	Total Intrusion Volume (mL/g)	Total Pore Area (m^2/g)	Median Pore Diameter (nm, Volume)	Median Pore Diameter (Area) (nm)	Average Pore Diameter (4V/A) (nm)	Porosity (%)	Stem Volume Used (%)
FL0	0.0664	5.825	102.3	14.7	45.6	14.23	39
FL5	0.0679	7.019	101.0	8	38.7	14.50	38
FL10	0.0809	8.610	95.8	8.9	37.6	16.75	48
FL15	0.0854	8.984	188.4	6.6	38	17.62	48
FL30	0.0905	10.559	243.3	5.9	34.3	18.50	50
FL50	0.1005	10.481	380.7	5.4	38.4	20.22	53

3.2. Radon emission behavior (open-loop)

Open-loop radon testing conducted using the RAD7 system over extended periods (up to 72 hours) revealed a steady increase in radon concentrations as fly ash content increased. The average radon level measured for the 0% fly ash sample was 20.8 Bq/m^3. This value increased consistently with increasing substitution, reaching 32.7 Bq/m^3 in the 50% fly ash sample. The background radon concentration measured in the laboratory environment was 19 Bq/m^3, which is considered typical for well-ventilated indoor air and was used as the baseline reference in this study. Radon emission from raw fly ash reached 26.7 Bq/m^3. Although both values remain below international guidelines (WHO: 100 Bq/m^3; EPA: 148 Bq/m^3), the increase of approximately 8 Bq/m^3 (~42%) is scientifically meaningful. This difference is statistically supported by repeated measurements and associated standard deviations, which confirm that the rise is not attributable to random variability. It is also important to note that indoor radon levels can vary geographically depending on local geology, particularly uranium and radium content in soil and rocks (Papastefanou, 2009). However, in this work, the test conditions were controlled, and measurements were designed to isolate emissions from the material itself rather than environmental background. Thus, the observed increase in radon emission is primarily attributed to the material composition and microstructure.

Open-loop test results for radon concentration levels from cement pastes with varying fly ash substitution are presented in Table 6, while the corresponding radon concentration graph— including the laboratory background level obtained from the RAD7 open-loop testing—is shown in Figure 4.

Table 6. Open-loop test results for radon concentration levels from cement pastes with fly ash substitution and raw materials

Sample Code	Fly Ash (%)	Average Radon Concentration (Bq/m^3)	Standard Deviation (±)
FL0	0	20.8	±1.1
FL5	5	23.1	±1.2
FL10	10	24.8	±1.3
FL15	15	26.3	±1.2
FL30	30	29.2	±1.5
FL50	50	32.1	±1.6
P1	0	21.2	±1.3
P2	100	26.7	±1.1
P3	0	25.2	±1.2
Room Air	—	19.0	±1.1

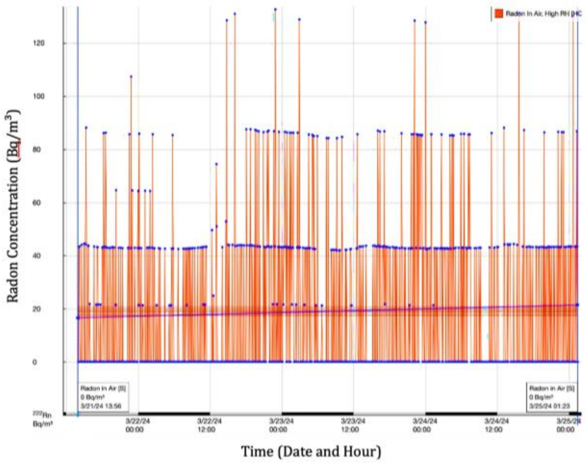

Figure 4. Graph of radon concentration in laboratory air measured with RAD7 under open-loop conditions.

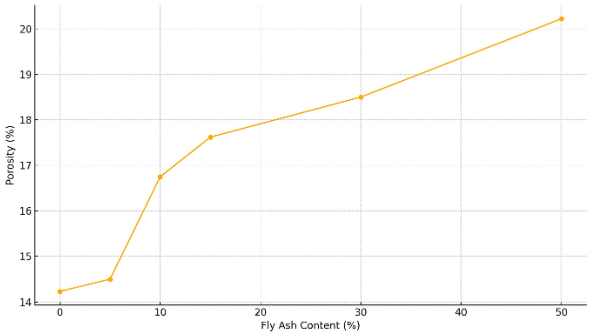

Figure 5. Porosity of cement pastes at different fly ash replacement ratios.

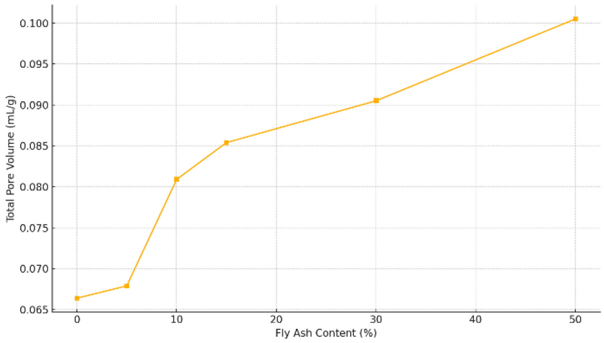

Figure 6. Total pore volume variation with increasing fly ash content.

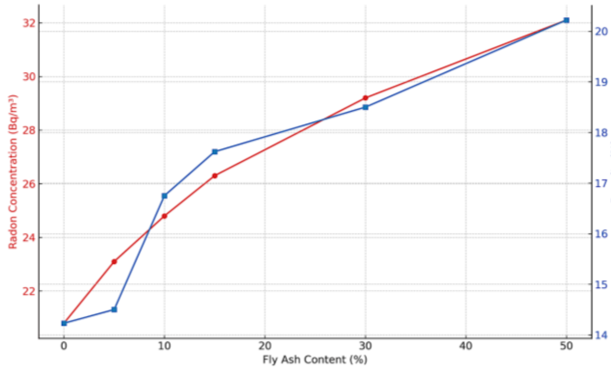

Figure 7. Effect of fly ash content on radon concentration (left axis) and porosity (right axis) after 28 days of curing.

4. Discussion

The experimental results demonstrate a consistent trend of increasing radon emission with higher levels of fly ash substitution in cement pastes, which is closely linked to alterations in the material's pore structure. Mercury intrusion porosimetry (MIP) revealed a rise in total porosity from 14.23% in the control mix to 20.22% at 50% fly ash. As shown in Figure 5, total porosity increases progressively with fly ash addition, reinforcing the structural weakening observed at higher substitution levels. This ~42% increase is attributed to the dilution and filler effects of fly ash, which reduce the quantity of cement clinker available for hydration (Hosseinpour and Osmanlıoğlu, 2024a). Consequently, the matrix at higher replacement levels contains more unhydrated or partially hydrated regions, resulting in more extensive capillary voids. The total pore volume increased from 0.0664 to 0.1005 mL/g, while internal surface area nearly doubled—from 5.825 to 10.481 m^2/g—indicating significant microstructural change. Figure 6 demonstrates the increase in total pore volume with fly ash content, supporting the development of a more open and interconnected pore network.

This shift also led to the formation of a bimodal pore structure. The volume-based median pore diameter expanded from ~102 nm to ~381 nm, reflecting an increase in large, percolating capillary pores. Meanwhile, the area-based median pore diameter decreased from ~14.7 nm to ~5.4 nm, indicating the presence of finer gel pores. The growth in large capillaries is linked to the inability of early-stage hydration to fill the original water-filled voids, while the finer pores are likely produced by ongoing secondary pozzolanic reactions. However, at 28 days—the testing age used in this study—Class F fly ash's pozzolanic reactivity remains limited (Mehta and Monteiro, 2014; Scrivener and Nonat, 2011). Therefore, the microstructure remains dominated by interconnected voids rather than refined gels (Diamond, 2000).

Radon concentration data collected using an open-loop RAD7 system showed a strong correlation with these structural changes. Concentrations increased from 20.8

Bq/m^3 at 0% fly ash to 32.1 Bq/m^3 at 50%. The inclusion of standard deviations for each measurement demonstrates that the observed trend is statistically consistent and experimentally reliable. Figure 7 illustrates the simultaneous increase in radon concentration and porosity with rising fly ash content.

This rise stems from two primary mechanisms. First, the increased radioactive source term due to fly ash's elevated radium-226 (Ra-226) content which is the immediate parent nuclide of radon-222 (Rn-222). As Ra-226 undergoes alpha decay, it generates Rn-222, a noble gas that can migrate through pore spaces and be exhaled into the surrounding air. Although direct Ra-226 measurements were not performed in this study, its presence is inferred from the uranium content, given their position in the decay chain. Second, the enhanced radon transport efficiency resulting from a more open and interconnected pore network (Osmanlıoğlu, 2019). In denser matrices, radon atoms often decay within the solid before escaping, whereas larger and more connected pores offer lower resistance to radon movement, enabling greater exhalation before decay.

Fly ash particles themselves also influence radon release. Their spherical morphology includes porous and hollow structures (e.g., cenospheres), which may either retain or emit radon depending on their pore connectivity. The near-linear increase in radon concentration with increasing fly ash substitution indicates that the added radium content was effectively mobilized due to the microstructure's increased permeability. In the open-loop test setup, this dynamic was clearly captured, as radon was continually measured in real-time, and its steady increase paralleled the structural evolution of the paste.

The findings help clarify the mixed conclusions found in the literature. Some studies have observed that fly ash can reduce radon emission when it contributes to a denser matrix or when the ash itself has a low radon emanation coefficient (Kumar et al., 2010; Taylor-Lange, Stegemann, and Weiss, 2014). For instance, pastes containing up to 60% fly ash showed lower emissions in some cases due to limited emanation or tighter microstructure. Taylor-Lange et al. noted that fly ashes with low radon emanation fractions (~1–2.5%) might even suppress radon output. However, these effects are contingent upon the ash's properties, replacement level, and degree of hydration.

In contrast, other studies—particularly those using high-radionuclide fly ash—report increased radon release. Osmanlıoğlu (2021) found that using lignite-based Class F fly ash led to elevated radon emission, especially at higher substitution levels. Our study supports this trend. Despite the theoretical potential for radon retention in dense systems or in certain fly ash types, the real-world microstructure induced by 30–50% fly ash replacement tends to favor diffusion and emission. The added fly ash increased the supply of radium-226 while simultaneously opening up the network for radon escape. Thus, the increase in both source and transport efficiency explains the consistent rise in radon emission. This correlation is clearly captured in Figure 7, which combines both radon concentration and porosity data, highlighting the microstructural role in facilitating radon diffusion through the hardened matrix.

It is important to consider the role of curing time. Pozzolanic activity can refine the microstructure over long durations, reducing capillary porosity and potentially radon transport pathways. However, most practical applications use cementitious materials within 28 to 56 days, limiting the timeframe for such refinement. At these ages, the microstructure is still evolving, and the fly ash-induced porosity remains relatively high. Our data suggest that while modest additions (5–15%) result in limited increases in porosity and radon release, higher levels (≥30%) lead to pronounced structural coarsening and a significant rise in radon exhalation.

This dual effect poses a challenge for sustainable construction. Fly ash is widely promoted for its environmental benefits—it reduces clinker demand, lowers CO_2 emissions, enhances workability, and minimizes thermal cracking. From a materials management perspective, its use also addresses waste recycling. However, increasing fly ash beyond moderate levels can compromise indoor air quality by increasing radon concentrations —a recognized health risk and the second leading cause of lung cancer in non-smokers (Field et al., 2007; World Health Organization, 2010).

While the radon levels measured in our test environment (20–32 Bq/m^3) fall within acceptable indoor limits, their relative increase of ~50% in fly ash-rich pastes cannot be ignored. In a real building, this could contribute to a cumulative elevation in indoor radon, particularly in spaces with limited ventilation or poor sealing. Surface area exposure, air circulation, and underlying soil gas pressure also influence how much material-derived radon contributes to indoor air concentrations. Therefore, even moderate material emissions can become significant when scaled to full interior volumes.

To mitigate these risks, a combination of strategies should be considered. Limiting fly ash substitution to below ~30% may provide a good compromise between sustainability and health safety. When higher replacements are necessary—due to cost, availability, or performance goals—complementary measures such as surface sealants, radon-absorptive additives, or improved ventilation systems should be implemented. Additionally, blending fly ash with other supplementary cementitious materials (e.g., silica fume) may help refine the pore network and counteract the radon-enhancing effects.

Finally, it may be appropriate for construction standards and material certifications to include radiological performance benchmarks. Regulations could require maximum allowable Ra-226 content or set limits on radon exhalation rates, especially for materials used in indoor applications. A mechanistic understanding—linking composition, hydration, and pore evolution—is key to predicting and controlling radon behavior. This study demonstrates that effective material design must account for both the radioactive source potential and the structural pathways that govern emission.

In conclusion, while coal fly ash contributes significantly to sustainable construction practices, its influence on microstructure and radon emission requires careful evaluation. By considering both short-term curing effects and long-term performance implications, engineers can make informed decisions about substitution levels and mitigation approaches. Balancing environmental goals with public health protection is not only possible—it is essential for responsible material innovation in the built environment.

5. Conclusion

This study presents a comprehensive assessment of how Class F fly ash influences radon emission and microstructural properties in cement pastes, emphasizing microstructural changes. By substituting Portland cement with Class F fly ash at 0–50% levels and utilizing mercury intrusion porosimetry and open-loop radon testing, a direct link was identified between pore evolution and radon release behavior.

Key findings reveal that increasing fly ash content leads to elevated porosity and notable changes in pore size distribution. At 50% substitution, porosity rose to 20.22% from 14.23% in the control, and internal surface area nearly doubled, indicating a more open and connected pore network. These structural shifts significantly influence radon exhalation: average radon concentrations, rising from 20.8 Bq/m^3 in the control mix to 32.1 Bq/m^3 at 50% replacement. Intermediate substitutions (5–30%) showed a stepwise increase, demonstrating a strong correlation between fly ash dosage and radon emission.

The rise in radon release is attributed to two interrelated mechanisms. First, Class F fly ash inherently contains more radionuclides, including radium-226, than Portland cement. Second, higher substitution levels produce less dense matrices, enhancing radon diffusion through the pore network. While pozzolanic reactions may eventually refine the structure, at 28 days these effects remain limited, and the increased permeability dominates the behavior. Consequently, any potential radon retention offered by secondary gels is insufficient to counteract the openness of the network.

These results help identify optimal substitution thresholds. Fly ash levels of 15–25% appear acceptable, causing only modest porosity increases and a manageable radon rise (~5 Bq/m^3 at 20%). If sufficient curing occurs, these systems may densify further. However, beyond 30%, the microstructure becomes significantly more porous, and radon emissions rise markedly—up to 50% above the control at 50% substitution. Such levels can be problematic when scaled to full buildings. Thus, fly ash content around 25–30% may mark a practical limit, beyond which careful justification and mitigation are needed. It should be noted that the observed increase in radon emission may be influenced by the specific characteristics of the fly ash used in this study, which was sourced from the Tunçbilek thermal power plant. Therefore, the findings may not be directly generalizable to fly ash from other sources with different radionuclide content.

In conclusion, using coal fly ash in cement paste supports sustainability goals but must be balanced against indoor environmental risks. Fly ash enhances workability, reduces clinker use, and lowers emissions, but high contents increase radon exhalation. A strategic approach is recommended: moderate substitution levels, extended curing, and microstructural control. Future research should explore long-term densification, combinations with other SCMs, and source-specific behavior. Additionally, strategies like surface coatings or radon-absorptive admixtures should be considered. Regulatory frameworks might also integrate radon performance benchmarks to ensure recycled materials do not compromise occupant safety. Ultimately, balanced strategy involving moderate substitution, extended curing, and microstructural control is recommended.

Author Contributions

The percentages of the authors' contributions are presented below. All authors reviewed and approved the final version of the manuscript.

	A.H.S.	A.E.O.
C	60	40
D	55	45
S	50	50
DCP	60	40
DAI	50	50
L	55	45
W	65	35
CR	50	50
SR	70	30
PM	50	50
FA	50	50

C=Concept, D= design, S= supervision, DCP= data collection and/or processing, DAI= data analysis and/or interpretation, L= literature search, W= writing, CR= critical review, SR= submission and revision, PM= project management, FA= funding acquisition.

Conflict of Interest

The authors declared that there is no conflict of interest.

Ethical Consideration

Ethics committee approval was not required for this study because of there was no study on animals or humans.

Acknowledgements

This study is derived from the author's doctoral dissertation and forms part of the PhD research conducted within the Department of Mining Engineering, Faculty of Engineering, Istanbul University–Cerrahpaşa. The author sincerely thanks his thesis advisor, Prof. Dr. Ahmet Erdal Osmanlıoğlu, for his scientific contributions, guidance, and unwavering support.

References

Blissett RS. 2012. A review of the multi-component utilization of coal fly ash. Fuel, 97: 1-23.

Diamond S. 2000. Mercury porosimetry: Porosity or artifact? Cem Concr Res, 30: 1517-1525.

EPA. 2023. Health risks of radon. United States Environmental Protection Agency. URL: https://www.epa.gov/radon/health-risk-radon (accessed date: April 8, 2025)

Field RW, Krewski D, Lubin JH, Zielinski JM, Alavanja M, Catalan VS, Klotz JB. 2007. An overview of the North American residential radon and lung cancer case–control studies. J Toxicol Environ Health A, 70: 1882-1889.

Hosseinpour Sheikhrajab A, Osmanlıoğlu AE. 2024. Comparison of radioactivity concentration levels of coal and lignite used in major thermal power plants in Turkey. In: Proceedings of the 10th International Artemis Scientific Research Congress, April, Romania, pp:59-96.

Hosseinpour Sheikhrajab A, Osmanlıoğlu AE. 2024a. The effect of Tunçbilek Thermal Power Plant waste fly ash on mechanical properties of Portland cement. Nat Appl Sci J, 7: 40.

Hosseinpour Sheikhrajab A. 2025. Determination of radon emission in cements made with coal fly ash. PhD thesis, Istanbul-Cerrahpaşa University, Institute of Engineering, Istanbul, Türkiye, pp: 115-175.

Kumar A, Chauhan RP, Dahiya N. 2010. Radon exhalation rate in fly ash and fly ash blended cement. Radiat Meas, 45: 223–226.

Mehta PK, Monteiro PJM. 2014. Concrete: Microstructure, properties, and materials. McGraw-Hill Education, New York, USA, pp: 646.

Osmanlıoğlu AE. 2019. Natural radioactivity in Turkish coal-fired power plant ashes. J Environ Radioact, 208-209: 106021.

Osmanlıoğlu AE. 2021. Evaluation of radiological risks from coal combustion residues used in building materials. Constr Build Mater, 270: 121473.

Papastefanou C. 2009. Radon in ambient air and soil gas in the vicinity of uranium mining and milling facilities. J Environ Radioact, 100: 385-392.

Righi S, Bruzzi L. 2006. Natural radioactivity and radon exhalation in building materials used in Italian dwellings. J Environ Radioact, 88: 158-170.

Scrivener KL, Nonat A. 2011. The chemistry of cement hydration. Cem Concr Res, 41: 651-665.

Taylor-Lange SC, Stegemann JA, Weiss WJ. 2014. Assessing the transport properties and radon emanation of concrete containing fly ash for radioactive waste encapsulation. Cem Concr Compos, 53: 103-113.

World Health Organization. 2010. WHO handbook on indoor radon: A public health perspective. WHO Press. URL: https://apps.who.int/iris/handle/10665/77945 (accessed date: March 10, 2025)

Yüksel İ, Göncüoğlu MC. 2011. Utilization of high volumes of Turkish fly ashes to produce sustainable construction materials. Constr Build Mater, 25: 1610-1618.

Zhang MH, Malhotra VM. 1996. High-performance concrete incorporating rice husk ash as a supplementary cementing material. ACI Mater J, 93: 629-636.